RRFM 2008

Transactions

2.3. -5.3. 2008
Hamburg, Germany

European Nuclear Society
Rue de la Loi 57
1040 Brussels, Belgium
Phone + 32 2 505 30 54
Fax +32 2 502 39 02
E-mail info@euronuclear.org
Internet www.euronuclear.org

ISBN 978-92-95064-04-1

These transactions contain all contributions submitted by 29 February 2008.

Session V

Innovative methods in research reactor analysis

MONTE CARLO CORE CALCULATION FOR A MIXED TRIGA HEU/LEU CORE

T. STUMMER, R. KHAN, H. BÖCK, M. VILLA
Vienna University of Technology, Atominstitut
Stadionallee 2, 1020 Vienna – Austria

ABSTRACT

The TRIGA reactor Vienna operates since March 1962 at the rather low power of 250 kW and with a completely mixed core using two types of LEU and one type of HEU elements since 1974. This makes a detailed core calculation difficult especially as many relevant data for MNCP calculation were not always readily available. Further there are only very few TRIGA reactors with such a core composition. In the absence of good burn up and temperature data for the core a parametric study with all fresh fuel and averaged fuel temperature for different fuel element mixes was done. This includes thermal/fast flux, hot rod factor and k_{eff} estimation for an all 102, a 102/104 mixed and a 102/104/FLIP mixed core. The model was run using MCNP 5.14 together with the ENDF/B-VI.5 library

1. Introduction

In the US spent fuel return program the DOE places great emphasis on getting HEU fuel elements replaced by LEU elements in research reactors. At the TRIGA reactor Vienna this means looking for options to replace nine 70% enriched fuel elements and the possible effects on the reactor in case of such a replacement. To estimate the changes a MCNP model was developed and applied to get core parameters for different core configurations. The model and its results will be presented in more detail in this paper.

2. Reactor Configuration

At the Atominstitut, Vienna, Austria, the 250 kW TRIGA Mark-II reactor is mainly used for nuclear education and training in the fields of neutron- and solid state physics, nuclear technology, reactor safety, radiochemistry, radiation protection, dosimetry, low temperature physics and fusion research. It is equipped with two thermal columns, four beam lines and three in- core pneumatic transfer systems. The core has a cylindrical grid plate with 96 positions in 6 rings for fuel elements, three control rods and various other core installations with the same outer diameter of a standard TRIGA fuel element. First criticality of the reactor was achieved 1962 with 62 standard TRIGA fuel elements (20% enriched) and fuel elements have slowly been added (to a total of 82 today) since then to account for burn up. General Atomics, fuel supplier, has changed the fuel specifications several times during this period, which led to a mixture of types in a many of the TRIGA reactors. Currently three types of fuel elements are used in the TRIGA Vienna with the details seen in table 1. Most of the 54 elements of the Al-clad type 102 have been in the core since the initial start of the reactor operation and have a correspondingly high burn up rate. The 19 type 104 elements have been added incrementally since the late 60-ies and therefore vary strongly in burn up. In 1972 the nine 70% enriched elements (called FLIP = **F**uel **L**ifetime **I**mprovement **P**rogram) were added and are the main reason for this work. Originally this type was designed for high powered TRIGA reactors in continues operation. Due to the operation schedule (only 8 hours per working day) and low power of the TRIGA Vienna together with the high burnable poison

content they have not yet reached their maximum reactivity value after 36 years while providing a significant reactivity contribution.

Fuel element type	102	104	110 (FLIP)
Fuel moderator material	U-$ZrH_{1.0}$	U-$ZrH_{1.65}$	U-$ZrH_{1,65}$
Uranium content (wt%)	8.5	8.5	8.5
Enrichment (%)	20	20	70
Average ^{235}U content (g)	38	38	136
Burnable poison	SmO_3-disk	Mo-disk	Erbium 1.6 wt%
Diameter of fuel meat	35.8 mm	36.3 mm	36.3 mm
Length of fuel meat	35.6 mm	38.1 mm	38.1 mm
Graphite reflector length	10.2 mm	8.73 mm	8.81 mm
Cladding material	Al-1100F	304 SS	304 SS
Cladding thickness	0.76 mm	0.51 mm	0.51 mm

Tab 1: Specifications of fuel elements used in the core of the TRIGA reactor Vienna

3. MCNP Model

The part of the reactor, which is modeled, consists of a cylinder with a height of 120 cm and a radius of 96.5 cm centered at the middle of the core. In the radial direction this corresponds to the core with reflector, beam lines, thermal and thermalising column up to the Al reactor tank walls, and axially to about 25 cm of water above and below the fuel elements. Figure 1 shows a horizontal cross section of the MCNP model.

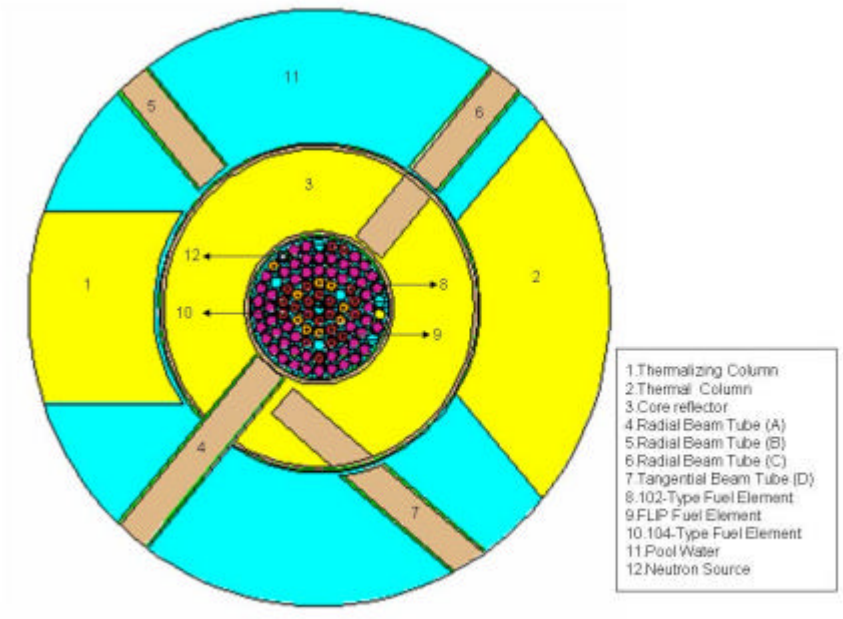

Fig 1: Horizontal cross section of the TRIGA Mark II core in Vienna

Due to lack of accurate data several assumptions had do be made:

- The core is at room temperature, corresponding to very low power operation because the fuel meat temperature at full power operation is unknown.
- All fresh fuel is used because of the lack of reliable burn up data.
- For each fuel element type an average element was assumed and used.

The last point has bigger implications than it seems at first glance. Not only does the ^{235}U content differ +/- 0.5g per element (avg. 38g) according to the shipping papers but more importantly the hydrogen to zirconium ratio differs markedly (from 1.57 to 1.63 for the nine FLIP elements). Even relative minor shifts in the ratio have a significant effect on k_{eff} simulations because most of the neutron moderation happens inside the fuel: For example changing the H-content from 1.6 to 1.65 (+0.0484 wt% with both values found in data sheets for the same elements) for the 104 elements (19 out of 82) results in a k_{eff} change of +1.12%. Additionally the control rods were left out of the model to eliminate them as an error factor resulting in a direct calculation of the excess reactivity.

4. Methodology and Results

Using the kcode option of MCNP the above model was run in three different configurations: First an all type 102 element core according to the original core map of 1962 was used to validate the model with the historic reactor logs. This resulted in a simulated excess reactivity within 0.2 $ of the historical value, which is reasonable when taking an error of up to +/- 10% into account for the rod calibration values in 1962. Following the validation two configurations based on the current core map (as seen in Fig. 1) were considered: one with the HEU FLIP elements in place and one with 104 elements instead of FLIP. For each case the results of the k_{eff} estimation (MCNP standard deviation < 0.00005 in all cases) and the hot rod factor defined as maximum element power divided average element power (values obtained through F7 tallies) are given below in table 2.

Core configuration	1962	Current core	Current core without HEU
Number of type 102 elements	62	54	54
Number of type 104 elements	0	19	28
Number of FLIP elements	0	9	0
k_{eff}	1.015	1.055	1.037
Hot rod factor	1.60	2.11	1.72
Position of hottest element	B2	C7	B2
Type of hottest element	102	FLIP	104

Tab 2: k_{eff} and hot rod factor for various core configurations

As explained above the use of fresh fuel elements in the model together with an 82 element core map gives a highly super critical core but the difference between the FLIP and the all LEU core gives an idea about the effects of mixing HEU and LEU elements. Because of the different burn up behavior of FLIP and standard elements the differences are actually understated in the simulations. By experimentally replacing a FLIP fuel element in the C ring by a standard stainless steel fuel element the change in reactivity by a an all LEU core can

be estimated to -2.4 $ compared to -2.25 $ in the simulation. The same ratio between experiment and simulation should be true for the hot rod factor in the cold core. At full power operation the strong negative temperature feedback of zirconium hydride fuel should decrease the hot rod factor for each individual core configuration and additionally reduce the differences between the configurations somewhat. The following two figures were created by comparing plots of neutron flux mesh tallies for the FLIP and LEU core configurations at certain energy ranges. Note that each core plot was normalized to the highest flux on the individual plot, giving only comparable flux shapes not the relative strength between the configurations.

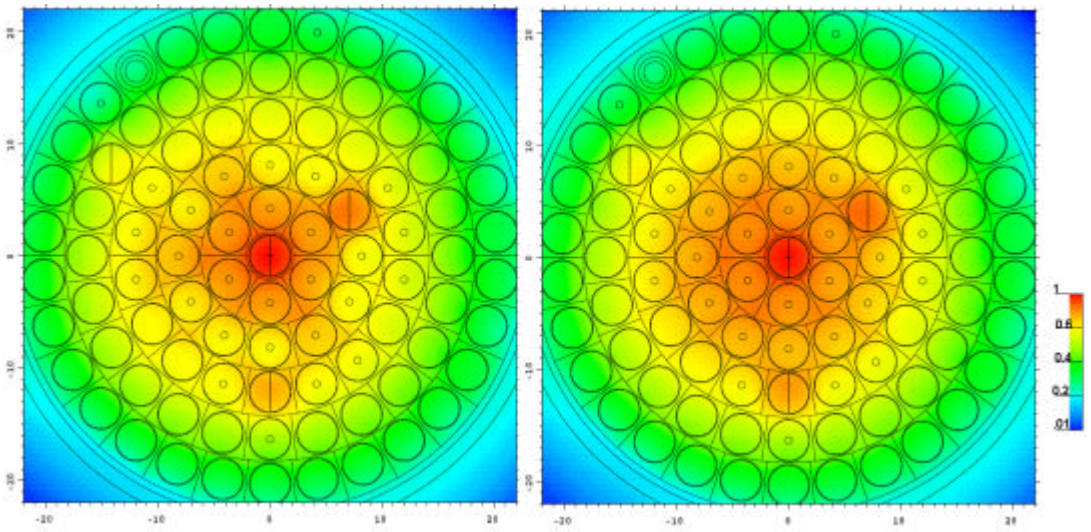

Fig 2: Total neutron flux renormalized to the maximum for FLIP core (left) and LEU core (right)

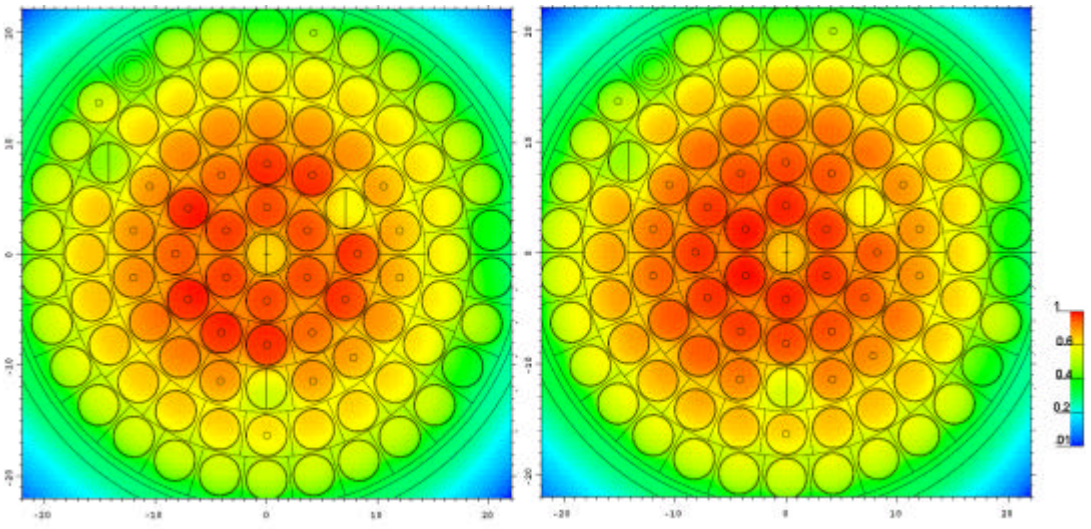

Fig 3: Fast neutron flux (E>0.2 MeV) renormalized to the maximum for FLIP core (left) and LEU core (right)

The positions with a vertical line through them are filled with water and correspond to the central thimble tube and the three control rods. These show a higher total flux than comparable positions, which is caused by a slightly too coarse mesh grid increasing the effects of mechanic of the calculation. MCNP calculates the flux in this type of tally by dividing the total track length of neutrons through the volume of a mesh box. This averages

the flux over the volume and so will lead to skewed results if comparing two regions with very different absorption cross sections, unless the grid size is well below the mean path length in both materials. The left part of figure 3 shows clearly the high reaction rates in the nine FLIP elements in C-ring (the ninth FLIP is in the outermost ring). Interestingly the total flux in figure 2 shows no peaks at the FLIP positions because the depletion of the neutron flux in the thermal region due the high ^{235}U and burnable poison content compensates the increase in the fast region. This effect demonstrated by gold activation around the FLIP positions.

5. Outlook

Current research of the reactor group is going in two directions with MCNP in Vienna. One is to improve the presented model to account for burn up. The necessary data should be provided by burn up calculations and gamma spectroscopy measurements of the fuel. The other one is to use the model as a basis for flux and activation calculation in the surrounding concrete shield in order to estimate the amount of waste at the decommissioning of the reactor. Further it is planned to use a Cerenkov glow camera to determine the power rate of individual fuel elements.

6. Summary and conclusions

Unsurprisingly the calculations show that a homogenous LEU core has a better cosine formed flux distribution and a reduced hot rod factor compared to a mixed HEU/LEU core. Although this is positive, it is not particularly important in a 250 kW TRIGA reactor and the long term burn up behavior favors the current mixed core

7. References

1 J. F. Briesmeister, Ed. *MCNP – A General Monte Carlo N-Particle Transport Code, Version 5*, Manual, April 2003

2 H. Böck, *Possibility of a partial HEU-LEU TRIGA fuel shipment*, RRFM 2007, Lyon March 2007

3 General Atomic, *TRIGA Mark II Reactor General Specification and Description*, Reverence, GA-2627, March 1964

4 Reactor log book TRIGA Vienna, 16. March 1962

HIGHLY DETAILED TRIANGULAR MESH DIFFUSION THEORY VS. MONTE CARLO: MODELLING THE MIT RESEARCH REACTOR

ARNE P. OLSON
Argonne National Laboratory
9700 S. Cass Avenue, Argonne, IL 60439, USA

THOMAS H. NEWTON, JR.
MIT Nuclear Reactor Laboratory
138 Albany St., Cambridge, MA 02139, USA

ABSTRACT

The MITR is undergoing analysis studies for conversion from HEU to LEU. A detailed spatial model was needed for use in REBUS. The HEU fuel element has 15 flat plates within a rhombus, making its geometry only realizable in triangular-z neutronics codes, or in full complexity via Monte Carlo methods. The REBUS-PC/DIF3D input processor was modified to create a unique and highly detailed triangular-z model in twelve planar sections. The core is split by three aluminium webs at 120°. Three central fuel positions are enclosed in a hexagonal aluminium box. Six control blades, one control rod, and end fittings and reflectors all fit very well into the triangular-z model. A hemispherical vessel bottom cap is also modelled. Excellent comparisons of power distributions, control blade worth curves, and burnup reactivity predictions between REBUS-PC, and MCNP show that diffusion theory is not ready to be abandoned.

1. Introduction

The 5 MW MIT Research Reactor (MITR) is undergoing redesign studies within the GTRI/RERTR Program, to convert from 93 % HEU to LEU. The reactor is light-water-cooled, with a heavy water radial reflector inside a two-ring graphite reflector. Key design decisions on LEU fuel type, and the number of fuel plates per assembly, must soon be decided based upon parametric design studies using the REBUS-PC, MCNP and REBUS-MCNP codes. A typical core layout with 4 dummy fuel assemblies is shown in Fig. 1.

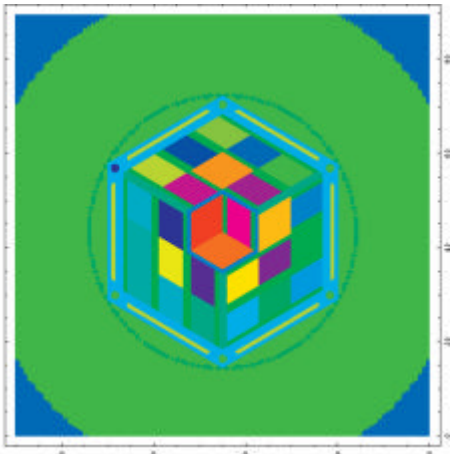

Fig. 1. MITR, Central Portion with 4 Dummies In Locations A-1, A-3, B-2, B-4

The HEU fuel element has 15 flat plates within a rhombic cross section, making its geometry only realizable in existing triangular-z neutronics diffusion theory codes, or in full complexity via Monte Carlo methods. The REBUS-PC/DIF3D code [1-2] input processor was extensively modified in order to create a unique and highly detailed triangular-z model containing more than 6.4 million elements. The full-core 3D model of MITR Core 2, consisting of 22 HEU assemblies and 5 solid aluminium dummies was developed in twelve planar sections. Each fuel assembly is homogenized across the x-y plane, but is split into 6 axial segments in order to enable a special fuel shuffling requirement that consists of flipping the fuel end-for-end. This improves fuel utilization, because the axial power shape is quite asymmetrical. The reactor core structure is hexagonal, but the core is split by three webs at 120 degrees. The central three fuel element positions are enclosed in a hexagonal aluminium box, sometimes used for fixed absorbers. Six control blades, one vernier control rod, and various end fittings and reflectors all fit very well into the triangular-z model. A hemispherical vessel bottom cap is also modelled.

It is very convenient in the model to make the rhomboid-shaped fuel assembly unit cell contain 8x16 mesh triangles. The optical thicknesses of the structural webs and the central aluminium box

are maintained in the model by adjusting their atom densities slightly to account for the wall thickness errors introduced by the mesh triangle size not quite matching the physical dimensions. This reactor is extremely challenging to model, both geometrically, and spectrally. For example, there is a very large variation in fast/thermal flux ratio in the three core rings, as well as in the vicinity of the light water, heavy water, and graphite reflectors. The effect of control blade position is also very large. Excellent comparisons of power distributions, control blade worth curves, and burnup reactivity predictions between REBUS-PC, MCNP and REBUS-MCNP show that diffusion theory is not ready to be abandoned.

2. Geometrical Modelling in Triangular-Z

Many research reactors use fuel elements contain flat plates to attain excellent physics and thermal-hydraulics performance. The MITR is unique because its fuel elements are rhomboid-shaped. Because three rhomboidal elements can be arranged into a hexagon, the MIT reactor combines features of flat, rhomboidal, and hexagonal shapes. In addition, radial boundaries created by vessel walls and by reflectors are circular. To make things even more complex, the vessel lower cap is hemispherically shaped. All of these features can readily be modelled in the Monte Carlo code MCNP. But what about deterministic, finite-element codes such as DIF3D?

Although DIF3D was created by ANL initially for fast breeder reactor applications, it has been a key component of the REBUS-PC code (and earlier versions of REBUS) since its inception in the 1960's. DIF3D has also evolved over this time into a general-purpose solver of multigroup transport theory with a variational nodal option in Cartesian and hexagonal geometries. It also has been used for sub-critical "burner" facilities driven by proton beams. Of interest for this work is its original capability to solve diffusion theory problems in hexagonal-z geometry with the finite-difference approximation, including upscattering. Three options are available: full core; third core symmetry in plane; and sixth core symmetry in plane. The triangular mesh for the full core option is contained within a rectangular domain of solution. All interior equilateral triangles are of the same size, with half-triangles needed on the two sides. This is the option best suited to the MITR, because it has not historically been operated with any core symmetry. Furthermore, there is a single regulating rod that destroys symmetry in the x-y plane.

For the axial mesh, we desired to have sufficient mesh intervals to have six axial layers in the active fuel length. This would enable burnup calculations to account approximately for the non-symmetrical axial flux profile, and would enable matching the operational tactic of taking partially-burned fuel out of the reactor, flipping it end-for-end, and reinserting it. Computing time would increase approximately linearly with the axial mesh size.

At ANL, we construct input geometry for DIF3D using the General Neutronics Input Processor, GNIP4C. When this work began, the only available capability in GNIP4C that used hexagonal-z geometry was one created for reactors using hexagonal-shaped fuel elements. This option was used in many fast breeder reactor design studies. But DIF3D itself was capable of solving any problem that could be given to it in standard binary interface file format GEODST, with macroscopic cross sections in binary interface file COMPXS. Hence the solution to the problem of how to use REBUS-PC/DIF3D for the MITR became clear: build a detailed representation at the level of every mesh triangle by creating a new option within the GNIP4C code.

The FORTRAN software planning began by realizing that geometrical components which appear in several places could be constructed by creating general-purpose subroutines to build each one as a template, and defining spatial offsets (that is, mesh triangles) to locate each desired component. Fuel elements come in three types: rhomboids arranged vertically, and horizontally in two orientations. There are 9 of each type. Three subroutines were needed to define the spatial mesh occupied by the 27 fuel locations, and to define the fuel element side plates.

As the geometry was studied, it was apparent that a very fine representation could be made assuming that the each fuel assembly consisting of15 fuel plates, associated interior cooling water channels, and side plates, fitted within 8x16 mesh triangles. Then the triangle size as determined by this match to the fuel cross sectional area would also provide a good fit to the three webs at 120 degrees that define the core arrangement outside the central hexagon. It also would fit well to the width of the central hexagonal structural element containing the central three fuel/dummy positions. We realized that computer power had increased enormously in recent years, making it possible to

construct quite large spatial meshes and still reach useful solutions in a reasonable time. We hoped for the ability to run burnup problems overnight. This objective was attained.

The overall hexagonal outer boundary of the reactor core would naturally follow in hexagonal –z geometry, by simply choosing to match as closely as possible the enclosed area. Similarly, the 6 control blades occupy rectangular slots that could be modelled as equivalent-area slots but with ends at 60 degrees, rather than at 90 degrees.

Circular boundaries such as the vessel wall, the inner graphite reflector, and the outer graphite reflector would be located in the spatial mesh in the x-y plane by locating the centroid of each triangle. If its radius was within a given spatial component, then the mesh point could be so identified. Any mesh triangles outside the outer radial reflector could also be identified. The DIF3D code ignores any mesh triangles outside the domain of solution. This is helpful to reduce computation time, because the overall circular shape of the domain of solution lies within a bounding nearly-square mesh. About 20% of the mesh is outside the outermost circular boundary. A final mesh size of (542,312,38) or 6.4 million elements was selected.

The reactor control blades are rectangular with a semi-circular end. A true spatial representation of this shape was not possible due to the need to limit the axial mesh to a reasonable size. An equivalent rectangular shape was used that preserved the area of the blade. This change must be accounted for when using the model, when the control blade tip is inserted to a particular location.

The reactor vessel bottom is a hemispherically shaped component. It has quite a large radius of curvature: 86.36 cm inner radius and 87.95 cm outer radius. It is properly modelled in the MCNP model, but it also is represented in the finite-difference model constructed for DIF3D.

The new version of GNIP4C, incorporated into REBUS-PC, required changing 10 existing subroutines, and adding 18 new subroutines to generate the new model. This new version of REBUS-PC retains the ability to solve all other non-MIT problems.

2.1 Key Dimensions of the Model

The entire reactor is located centrally within a mesh that is (542,312,38) in triangular, 3-dimensional geometry. To be properly aligned on the x-y plane, the number of mesh points in x and in y must be even numbers. The new input processor option will create the portion of the MITR model that lies within the given space. Initial development and testing took advantage of this capability to create only the small, central fuelled core in a (128,74,3) mesh. The physical coverage of the (542,312,38) mesh is 240.289 cm in x, and 240.002 cm in y. Any mesh triangle whose centroid lies outside a radius of 120 cm is excluded from the DIF3D domain of solution. The axial model consists of 7 uniform layers with 8,1,1,18,1,1,8 axial mesh intervals in them from reactor top to reactor bottom. Layer number 4 has 18 axial mesh intervals, which is further subdivided into six axial burnup zones of three nodes each. The number of axial burnup zones is a parameter that is coded in the FORTRAN model. Should more or less axial burnup zones be desired, it will be relatively simple to change one card, compile, and link to create a new executable.

The radial dimensions of circular features are:

1. graphite outer radius: 120 cm
2. vessel containing heavy water: outer radius = 61.595; thickness = 0.635 cm
3. vessel containing light water: outer radius = 26.035; thickness = 0.635 cm
4. radius between light and heavy graphite: 82 cm
5. radius between heavy water and aluminium ring, in top end box layer: 35 cm

The axial segments are:

Layer	Content	Start, cm	End, cm	Thickness, cm	Nodes
1	H_20	0	51.279	51.279	8
2	structure	51.279	55.089	3.81	1
3	end cap	55.089	60.01	4.921	1
4	fuel	60.01	116.85	56.84	18
5	end cap	116.85	121.77	4.921	1
6	vessel	121.77	124.77	3.00	1
7	D_2O	124.77	176.849	52.079	8

The Mesh Triangle side is 0.8883139 cm; the height is 0.7693015 cm. Its size is determined by the flat-to-flat dimension of the fuel, divided by the number of rows of triangles used in the model (8).

The Fuel Assembly occupies a flat-to-flat dimension of 6.15442 cm. There are 8 rows of triangles (points up) within this dimension, for an element oriented like A-1 or A-2. For elements oriented like B-1, the same number of triangles is assigned. Hence a lattice rhombus occupies 8 x 16 triangles. There are 6 rows of triangles assigned to contain fuel meat, clad, and water. The other two rows contain side plates and water. In order to preserve mass, one must scale the atom densities used for the fuel meat by the ratio of true cross section area/model cross section area. This also applies to any other area, such as side plate, hexagonal strut, fixed radial strut, etc. The cylindrical vessel walls are quite well modelled—within 2% of correct area—and need no correction.

2.2 Neutron Cross Sections

The RERTR Program has found that 7 neutron groups yields sufficiently accurate results for a variety of research reactors. This same set was chosen for the MITR work. Multigroup cross section sets were generated using the WIMS-ANL code [3]. Special care was taken in supercell models to account for the presence (or absence) of dummy fuel elements when generating fuel cross sections. A four-group library was also generated, but were not found to yield acceptable results. The use of more than 7 groups is a future option, but we are very satisfied with the quality of results obtained using 7 groups when compared to MCNP results.

2.3 Displaying and Verifying the Geometry

In order to create the model, it was necessary to find ways to plot the mesh structure. A “computer plot” was created initially to show the zone number assigned to each mesh interval, when aligned in a rectangular grid. This was fine for model development, but a display in true geometry was also needed to truly verify that individual components of the model were located correctly and had the correct boundaries. A plotting routine was created using *Mathematica* to plot every full or partial triangle in a given x-y plane. Different zones have different colours or shades. The figures shown in this paper were created by this routine.

3. Application of the Model to Modern PC’s

One key to success is: how long will it take to obtain a useful burnup solution? An early test of the 38 axial mesh model was solved in about 18 hours. The problem consisted on obtaining flux, power, reactivity, and burnup in 50-day time steps from 0 to 300 days. Thus each time point required about 2.6 hours. This problem was run under linux on a Xeon 3.8 GHz dual CPU machine. When run on a new machine using 2x Dual Quad 2.66 GHz chips, the running time is about 1 hour per time step. The 32-bit REBUS executable was created using Lahey/Fujitsu FORTRAN 95, where automatic parallelization and availability of multiple CPU’s was not requested of the compiler. It runs essentially on one processor. We still have some problems with the LF95 compiler, when we attempt to create a code that will take advantage of multiple CPU’s in the same box. Note: this capability to use multiple CPU’s exists now on linux, but is not yet available from Lahey/Fujitsu for Windows. The memory requirement is quite large at about 255 million double precision words. The job takes slightly more than 2 Gigabytes of memory, and runs at 98% efficiency as it is fully core-contained. Performance on linux machines with only 1 or 2 Gigabytes will be seriously degraded by paging. However, DIF3D has memory management options that can be used to reduce the memory requirement and eliminate the need for paging. Many scratch files are needed, and wall clock time is increased as more scratch files are used.

4. Refinements and Developments After Proof-of-Principle

There was a need for locating the control blades to match experimental measurements. This is now accomplished. Also, there could be anywhere from 25 dummies instead of regular fuel assemblies in some cores. The model generation process was changed to permit dummies to be anywhere in the 27 core locations. Key model dimensions could also be made user input parameters, by defining a new ARC System input data set such as A.MIT. This data set could

contain card types giving the mesh size, the axial mesh details, the location of dummies, and so on. For now, we create specific executables and INPUT files as needed.
If the number or locations of dummies changes, it is necessary to use the pre-existing ability of REBUS-PC to define a state-point showing the end-state dummy locations and the fuel contents. Then the job can be restarted, but using new dummy locations to build the geometrical model. The problem, unique to this detailed MITR model, is that the side plates have to be removed when a dummy replaces a fuel element. The dummies have no side plates. Removing (non-burnable) side plates cannot be accomplished automatically in REBUS-PC, but it is accomplished quite simply through creating the new state point configuration from existing output file information

Half-core symmetry in the x-y plane exists in the MITR if either there are no dummies, or there are three dummies in positions A-1, A-2, and A-3. If the fine-control regulating rod is out, and the above conditions for dummies apply, then there is 1/6th core symmetry. These symmetry conditions could apply until asymmetric fuel management operations take place. Due to the very long running time for DIF3D with the full core model, it may be advantageous to create symmetric models also. The 1/6th core model would run well, even on a 1 Gigabyte PC. One quantitative measure of the effectiveness of the overall REBUS-PC model is its ability to predict neutron flux and reactivity for any control blade (all 6 moved as a bank) position. Figure 2 shows excellent agreement between MCNP and REBUS-PC for the reactivity change with control rod bank position.

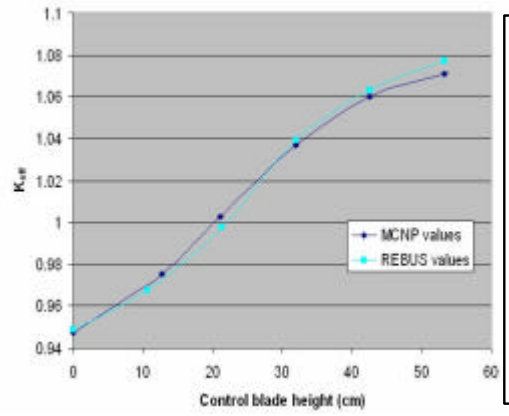

Fig. 2. Control Blade Worth Profile: HEU

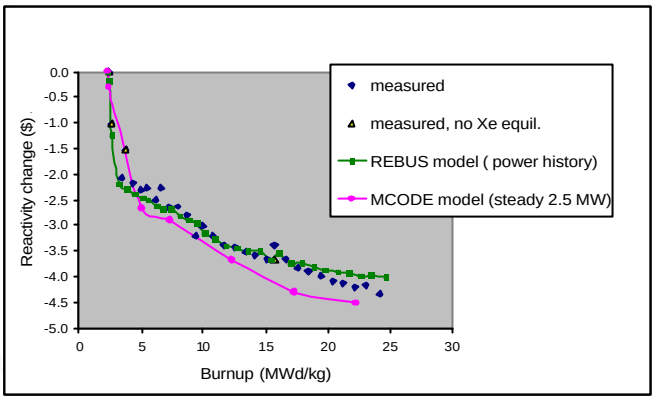

Fig. 3. Reactivity Change with Burnup: HEU

Figure 3 shows the result of a highly detailed simulation of the actual reactor operation as well as compared with steady 2.5 MW operation computed by the MCNP-ORIGEN code MCODE. It should be noted that the experimental reactivities have an uncertainty of about ± 0.1$, which arise from several components. We conclude:
1. The software and modelling design choices incorporated into the REBUS-PC diffusion theory model of the MITR yield accurate results;
2. The computational time is sufficiently fast to permit thorough design studies of new LEU cores;
3. REBUS-MCNP Monte Carlo burnup calculations, which take at least an order of magnitude longer to run than diffusion theory, will only be needed for final verification.

5. References

1. A. Olson, "A Users Guide for the REBUS-PC Code, Version 1.4," ANL/RERTR/TM-32, Argonne National Laboratory, December 2001.
2. K. L. Derstine, "RSIC CODE PACKAGE CCC-649, DIF3D 8.0/VARIANT8.0: Code System Using Variational Nodal Methods and Finite Difference Methods to Solve Neutron Diffusion and Transport Theory Problems," Provided by Argonne National Laboratory, Argonne, Illinois, March 2001.
3. J. Deen, W. Woodruff, C. Costescu, and L. Leopando, "WIMS-ANL User Manual Rev. 6," ANL/TD/TM99-07, Argonne National Laboratory, February 2004.

SOPHISTICATED NEUTRONIC CALCULATION OF THE ITER UPPER PORT DIAGNOSTIC SYSTEM USING MONTE CARLO METHOD

P. BOURAUEL, R. NABBI
Research Center Jülich
Leo-Brandt-Straße, 52428 Jülich - Germany

ABSTRACT

Research Center Jülich is involved in the development of a charge exchange recombination spectrometer (CXRS) for obtaining plasma parameters in the international fusion reactor ITER .For protection of the spectrometer from high temperatures and neutron flux, light from the plasma zone is guided through a mirror system and a glass fibre bundle. To perform nuclear analysis and to study the neutronic radiation load the Monte-Carlo-Code MCNP was employed. For this purpose a model with high fidelity of ITER and the Port Plug was used to acquire results of high accuracy. According to the results, the neutron flux at the first mirror is 7.3E+13 n/cm²s and decreases to 4.6E+7 n/cm²s at the back window. Due to continuous modification of the design a method was developed allowing flexible generation of the MCNP model and neutron transport simulation respectively.

1. Introduction

ITER (International Thermonuclear Experimental Reactor) is the international research and engineering proposal for an experimental project that will help to make the transition from today's studies of plasma physics to future electricity-producing fusion power plants. It will build on research done with today devices such as DIII-D, EAST, TFTR, JET, JT-60, TEXTOR, and will be considerably larger than any of them. The implementation of diagnostics on ITER will be a major challenge, as the environment will be much harsher. For example the levels of neutral particle flux, neutron flux and fluence will be respectively about 5, 10 and 10,000 times higher than in today's machines [1].

For the simulation of neutron transport in complex systems as the Port Plug structure of ITER different numerical methods are employed which are of deterministic or statistical character. Due to the complex geometry of ITER and the CXRS Port Plug encompassing inhomogeneous structures and components the MCNP Monte-Carlo-code has proven to be the solution for the study of the neutronic load on the components as well as for the calculation of the performance of the structures. The code is also extensively used worldwide in nuclear engineering to perform complex criticality studies and neutron and particle transport calculations [2].

Since the neutron flux distribution in the assembly is of importance to the operational performance of the components, lifetime, shielding performance and dose rate, detailed neutronic analysis and modeling are to be performed. In this work a sophisticated model was generated for the whole configuration of these components which was used for the determination of the flux distribution, nuclear heating and radiation damage.

2. Description of the CXRS Port Plug

ITER diagnostic equipment is integrated in six equatorial and 12 upper ports, five lower ports, and at many other locations in the vacuum vessel. The integration has to satisfy multiple requirements and constraints and at the same time must deliver the required performance.

The Charge Exchange Recombination Spectroscopy (CXRS) instrument analyses EM radiation in the visible region from the core and edge plasma regions in order to measure

important parameters like temperature profile, Helium ash density profile, Impurity density profile, plasma rotation, alpha particle confinement. The system will be installed at the upper port for measurements in the plasma core region. The CXRS system consists of the following subsystems: Collecting and re-imaging optics, fibre optic channels, spectrometers, detectors and data-acquisition.
Light emitted from the ITER plasma is collected by the front optics system. The light is guided through a labyrinth and imaged on the entrance surface of a bundle of fibre optic waveguides. Through the fibre optic waveguides the light is guided to a set of spectrometers of different types. The instrument will be installed in a port plug in diagnostic upper port #3. The upper port plugs are installed in the ITER Vacuum Vessel (VV) and includes a plasma-viewing first wall blanket shield module. Required mirror diameters are in the order of 35 cm which fits within the available cross-section of the port plug. However, design issues are seriously increased due to the following facts: The high amount of radiation in the front of the port plug precludes the use of transmissive elements, so that at the front opening only reflective optics can be used.
The first mirror is exposed to a high neutron and heat load and is in an environment where deposition of carbon is likely. Both leads to a high degradation rate of the first mirror and therefore protective measures are required to ensure the lifetime of the first mirror. Also the first mirror is exposed to large heat transients at the beginning of operation that may create a change in curvature of the mirror surface. The mirror material is one of the most important parameters to determine the rate of degradation. Presently the most likely option is to use a mirror made of mono-crystalline molybdenum. Furthermore, the mirror shall be placed in a retractable tube in order to be replaced after a while and a shutter will enable protection when CXRS is not functional between the shots. The shutter and the exchange construction are both mechanical moving systems. They should be simple in order to guarantee functionality. Fig. 1 shows the position of the CXRS port plug inside the ITER rector and the principle layout of the instrument. In order to separate the mechanical systems from the optical labyrinth, the periscope has been divided in a mechanical and an optical layer. The mechanical layer resides in the upper part of the periscope and consists of mirror 1, the shutter mechanism and the replacement system. The optical layer resides in the lower part of the periscope and consists of all optical elements except for mirror one. **Error! Reference source not found.**

3. MCNP Model

The MCNP Model of the ITER CXRS port plug is a complete 3-dimensional full-scale model with a high level of geometric fidelity representing a detailed geometrical nodalization like depicted Fig 1. In order to simulate the neutron movements as exactly as possible the port plug has been modeled with the surrounding zones in detail consisting of a whole 20° sector of the reactor. The MCNP model, consisting of 2400 geometrical cells, was provided by the ITER Team Garching. Side surfaces are reflecting for simulating all of the 360° torus. Cells, encompassing the neutron source, are located in the middle of the torus with a mathematical approximation of the real plasma neutron generation rate.
The geometry of the CXRS Port Plug was modeled separately and coupled with the ITER model. Due to the complex geometry and continuous modifications of the design, an efficient and flexible method had to be deployed to alter the model with the design process accordingly. For this purpose an algorithm was developed, allowing the calculation of geometrical configuration of the mirror system in accordance to the actual location, size and orientation. The program produces new cards for the angles and coordinate of the surfaces for inclusion into the MCNP input file without changing the structure of the input file. Different parametric studies were performed to examine the effect of design variation for optimal performance as well as the effect of gaps between the outer surface of the port plug on the shielding performance of its surrounding structures. Dependent on the version of the model the CXRS Port Plug consists of 20 or 130 additional cells.

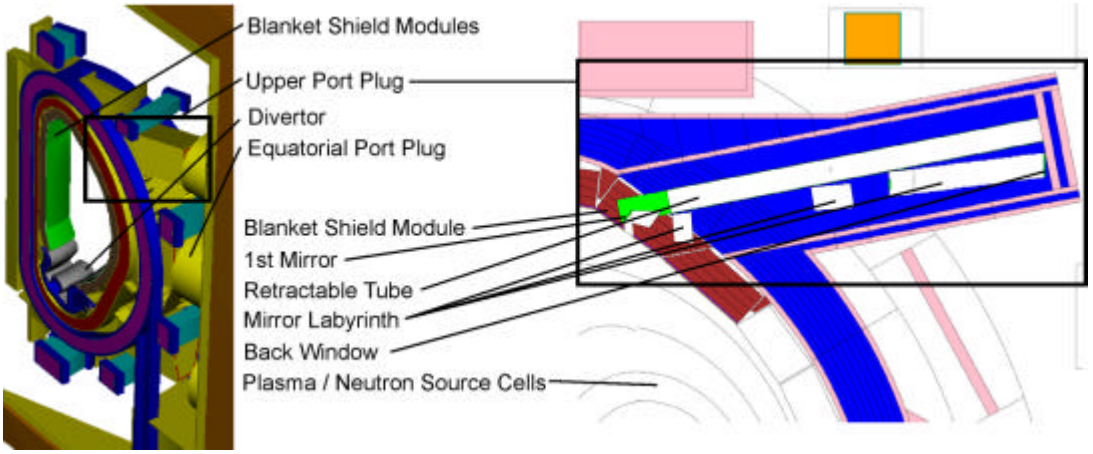

Fig 1: SABRINA plot of the MCNP model of the ITER 20° sector and a cut-away view of the CXRS Port Plug optical labyrinth with retractable tube for replacing the first mirror

Due to the shielding effects and large dimension of the model, only a small number of neutrons is tracked in the outer regions resulting in a high statistical relative errors on the calculated neutron flux. To improve the performance of the simulations, the variance reduction technique has been employed in some extend by the adjustment of cell importance. Number of neutron history was continuously increased to achieve a sufficient number of neutron tracks for a performed sampling including the outer regions of the Port Plug. The simulations have been performed on the massive-parallel computer system JUMP operated at the Research Centre Jülich.

4. Results of neutronic calculations

Due to the complexity of the geometrical model of the reactor and the large number of particle histories, the computing time was reduced significantly by the application of the parallel version of MCNP5. The simulations were carried out in steps of 1 million histories. After each step results were checked with regard to statistical errors and standard deviation and returned to MCNP by using the restart capability of the code. In total 15 Mio source particles were simulated resulting in a relative error (neutron flux) of less than 1 % around the front opening and less than 15% at the back windows of the structure. Tallies were introduced at the position of the mirrors for neutron flux and energy deposition. Additionally a row of fine mesh tallies (FMESH) was introduced to sample the areas around the mirrors, the Port Plug and ITER section. Some of the FMESH tallies were used to compute the nuclear heating by neutrons and gamma radiation in the respective material as well as the neutron damage in terms of atomic displacement. The resulting matrices were used for graphical visualization and the generation of 2D neutron flux and load patterns. A sequence of 75 matrices was combined to generate a 3D array for the neutron flux consisting of 420,000 voxels for further processing and visualization. For the verification purpose, a modified model was generated with for a former geometrical draft design of the Port Plug which was studied by a another group in the past. A comparison of the results (neutron flux and nuclear heating rate) for different mirrors in the whole port plug shows a very good agreement with the calculations reported in [4].
The calculations were performed for the new design with and without retracting tube which are compiled in Tab. 1. At the location of the first mirror in the model with retracting tube 7.30E+13 n/cm²s and 1.95 W/cm³ were calculated for neutron flux and nuclear heating respectively, representing the highest values in the Port Plug. Both values are comparable to that given in Ref. [4]. The neutron flux for the mirrors two and three is 4.53E+12 and 1.21E+13 n/cm²s respectively, showing an increase at the position of mirror three. This is due to the fact, that a higher fraction of neutrons is penetrating the shield and streaming to

the position through the optical labyrinth. The nuclear heating rate at the position of mirror 2 and 3 was calculated to be 1.11E-1 and 4.00E-1 W/cm³ respectively.

	Neutron Flux [1/cm²s]		Heating [W/cm³]	
	Retractable Tube	No Retractable Tube	Retractable Tube	No Retractable Tube
Mirror 1	7.30E+13	5.56E+13	1.95E+00	1.76E+00
Mirror 2	4.53E+12	4.13E+12	1.12E-01	1.07E-01
Mirror 3	1.21E+13	1.19E+13	4.00E-01	3.88E-01
Mirror 4	4.98E+10	4.95E+10	1.40E-03	1.22E-03
Mirror 5	3.42E+09	2.90E+09	4.97E-05	4.00E-05
Mirror 6	9.33E+07	3.50E+07	9.50E-07	5.60E-07
Mirror 7	2.19E+08	7.40E+07	5.60E-06	2.88E-06
Window	4.66E+07	1.58E+07	1.20E-06	6.28E-07

Tab 1: Results of the CXRS PP neutron flux and nuclear heating calculations using MCNP

For each following mirror, the neutron flux and heating decrease rapidly due to the shielding effect of the structures. An evaluation of the calculations for the model with retractable tube shows, that the relative error for the neutron flux remains below 10% for the first five mirrors and is lower than 15% at the last two mirrors including the back window. The values at the back window are 4.66E+7 n/cm²s for the neutron flux and 1.20E-6 W/cm³ for the nuclear heating rate.

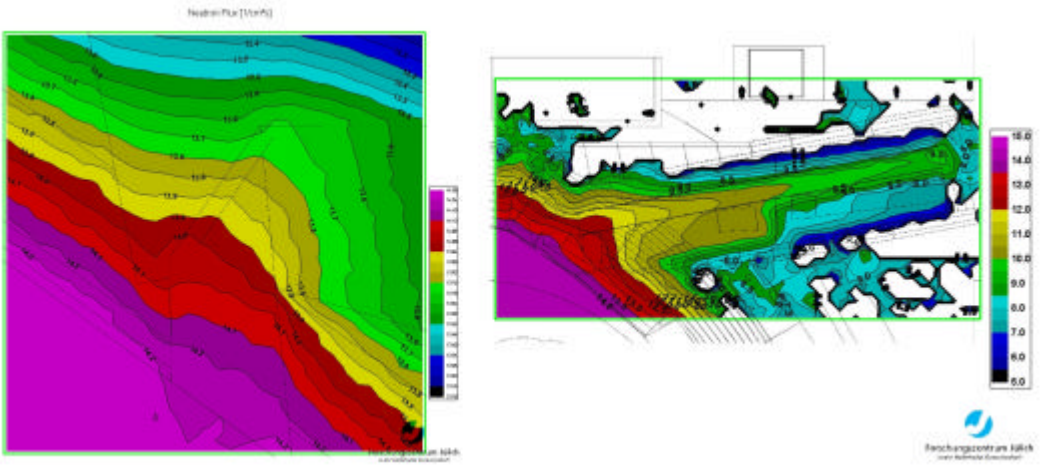

Fig 2: Results of the CXRS PP neutron flux calculations using MCNP [log(n/cm²s)] for the first mirror (left) and the whole assembly (right)

The distribution of neutron flux and heat load in the port plug system are given in Fig. 2 and Fig. 3. Left side of Fig. 2 shows the neutron flux distribution in the area around the first mirror. The values are varying inside the mirror with about one and a half order of magnitude. Visible is also the attenuation inside the materials. The right side of the Fig. 2 shows the neutron flux inside the structures of the whole Port Plug. Accordingly the maximum neutron flux appears at the rear part at the position of the retractable tube, which is modelled as a hollow cylinder to apply the worst case. The neutron flux at the window is about one order of magnitude lower. The comparison with the first configuration (with retractable tube) reveals that the use of a tube leads to significant effects to the flux at the back window. Fig. 3 displays the distribution of the neutron heating rate in the material zones. For the empty zones like the optical labyrinth and the retractable tube no values for the heating rate are displayed.

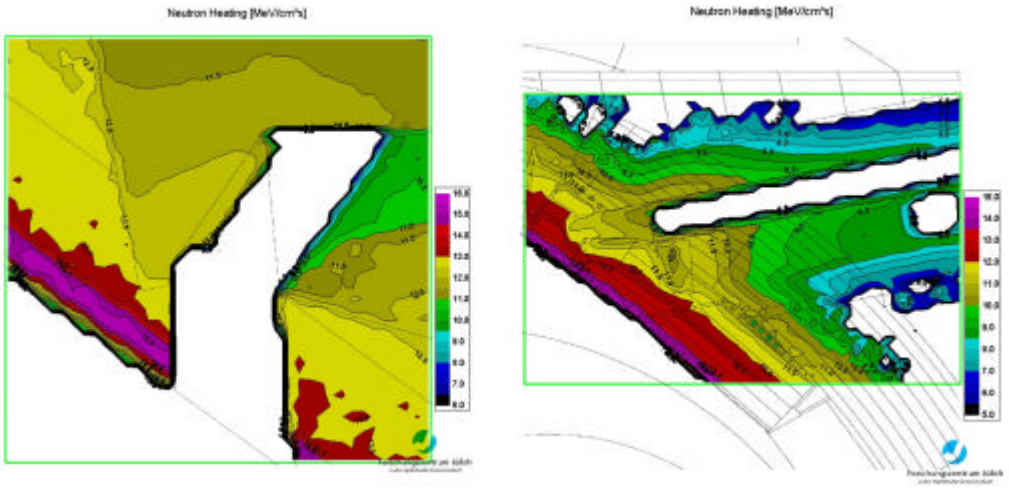

Fig 3: Results of the CXRS PP neutron heating calculations using MCNP [log(n/cm²s)] for the first mirror (left) and the whole assembly (right)

Additionally a model was created with gaps of different size around the port plug to account for streaming effect maybe caused by thermo mechanical stress. The calculation demonstrates, that gap size up to 2.5 mm only produces negligible effect on the neutron flux and heating at the rear structures and window, resulting from the shielding influence of the existing structures.

6. Conclusions

The work has shown that it is possible to calculate neutron flux and energy deposition in the whole Port Plug with sufficient precision. It is also shown, that MCNP models can be modified easily with existing tools to support frequent design modifications and parameter studies. Furthermore the presence of small gaps due to thermal expansion up to 2,5 mm are negligible because of the shielding effect of surrounding structures.

7. References

[1] COSTLEY, A.E., ET AL: THE CHALLENGE OF ITER DIAGNOSTICS, ECA VOL. 25A (2001) 1333-1336

[2] BRIESMEISTER, J.F.: MCNP 4A MONTE CARLO N-PARTICLE TRANSPORT CODE SYSTEM, RSICC, LOS ALAMOS, 1994, CCC-0200

[3] DI MAIO, M.; ET AL.: ITER CORE CXRS PROJECT, 2ND INTERMEDIATE REPORT, ITER-CXRS-CORE-FZJ-ESR-002-I1, JÜLICH 2007

[4] SHATALOV G.E., SHELUDIKOV, S.V.: UPPER PORT #3 NEUTRONIC ANALYSIS, MOSCOW 2002, REF NO. G55 MD 161 03-10-06 W 0.1.

APPROACH TO CRITICALITY IN THE BR2 REACTOR: MCNPX vs. POINT KINETICS METHOD

S. KALCHEVA, EDGAR KOONEN

SCK·CEN, Belgium Nuclear Research Centre
Boeretang 200, B-2400 MOL -Belgium

ABSTRACT

The behavior of the sub-critical core in the Belgian MTR BR2 during approach to criticality by withdrawal of the control rods is studied. The neutron source needed for the sub-critical counting is provided by the delayed neutrons from long-lived fission product decays in the burnt fuel assemblies and from the photo neutrons, released in (γ,n) – reactions on beryllium matrix. The three-dimensional Monte Carlo code MCNPX is used for evaluation of the k_{eff} values which are further introduced into the reactor kinetic equations to estimate the changes of the relative neutron density level in the sub-critical core. The calculations are performed and compared for two neutron source types: fission source (an eigenvalue calculation with neutrons starting from fuel assemblies) and external source, distributed in few burnt fuel assemblies around the core center. A simple method using MCNPX and point kinetics is proposed in support of the experimental technique for prediction of the counts in the detector (fission chamber) during critical approach by removal of the control rods.

1 INTRODUCTION

The approach to criticality in the different reactors can be done in a number of ways depending upon their design. A common procedure for the most heterogeneous reactors is approaching some sub-critical level (with control rods inserted at their lowest position) as function of uranium mass by loading the last fuel assemblies in consecutive fashion (one by one) into the reactor core. After that the approach to criticality is continued by withdrawal of the control rods so that the multiplication is increased to the level when the reactor becomes critical. The major start up problem is getting the reactor to a sufficient neutron flux level, so that the measuring instruments can detect it with reasonable statistic error. There are three basic ways to achieve the necessary initial flux level: (i) by inserting an extraneous physical neutron source into the reactor using (γ,n) or (α,n) – reaction (e.g., Ra-Be, Po-Be or Pu-Be sources); (ii) photo neutrons generated in (γ,n) – reactions on beryllium (this type of initial neutron source can be used in beryllium reflected reactors, although the intensity of the delayed photo neutrons is too low); (iii) delayed neutrons, emanating from long lived fission product decays in spent fuel assemblies (the intensity of these neutrons is sufficient for the start up measurements). The objective of this paper is to demonstrate how the approach to criticality in the BR2 reactor can be estimated using Monte Carlo technique vs. point kinetics, the last one being a basic method used in the measurements during critical approach. The final goal will be the application of the Monte Carlo code in support

and improvement of the experimental procedure executed at the approach to criticality. A simple method using MCNPX and point kinetics is proposed to be used for prediction of the counts in the detector (fission chamber) during critical approach by removal of the control rods.

2 APPROACH TO CRITICALITY IN BR2: EXPERIMENTAL PROCEDURE

2.1 Approach to criticality by uranium mass

The critical approach in the BR2 reactor is executed, following two consecutive stages. The first stage is approach to criticality as function of uranium mass (mainly ^{235}U, since BR2 uses 90% HEU fuel). Before executing this stage, almost the whole reactor core is loaded with the foreseen fuel elements and control rods, the last being inserted at their deepest position Sh=300 mm. The shutdown margin from Sh=300 mm to Sh=0 mm is about 3.5 $ for total control rods worth R0=12$, covering as well the loading of an additional reactive element as the ejection of the most efficient rod. The neutron source needed for the sub-critical counting is provided by the delayed neutrons from the decays of long-lived fission products, accumulated in the spent fuel assemblies and from the photo neutrons, released in the (γ,n) – reactions on beryllium. The six channels 'A' from the central crown, which are foreseen for the critical approach, are not loaded with fuel elements. Before the loading of every additional fuel element in channel 'A', three sub-critical counting are made to check the stability of the counting rates. As the approach to criticality is apt to be a very slow and careful one, the performance of the reactor is close to operation on the sub-critical multiplication formula. This means that the measuring instruments (fission chambers) are reading signal proportional to 1/(1-k). Then, the counting rate from a detector will be:

$$C_i = A\frac{1}{1-k} \tag{1}$$

Where: C_i is the counting rate; A is an instrument (detector) constant. As k approaches unity very slowly, the counting rate approaches infinity. The inverse counting rate C_0/C_i is calculated and plotted as a function of the additional fuel (C_0 is the initial measured counting; C_i is the counting measured after the loading of the i-the additional fuel element). An extrapolation is made to criticality, i.e. when $C_0/C_i=0$. The fuel element i+1 may be loaded only, if the extrapolation allows the loading at least of two additional fuel elements. After loading of all fuel elements, foreseen for the critical approach, the corresponding channels are locked This operation is done in critical approach if C_0/C_i is less than 0.30. As criticality is approached in this manner the reactor takes longer and longer to settle down to a fixed neutron level or counting rate. At criticality the reactor level will continue to rise indefinitely, because of the additive neutrons from the source.

2.2 Approach to criticality as a function of the control rods position

An examination of the changes of the power level in the sub-critical reactor with increase of k_{eff} toward unity by removing the control rods is performed. A neutron detector (fission chamber) is used to measure the neutron density as the reactor gets from one to another equilibrium level for each position of the control rods. Sub-critical counting are made on the four start-up pulse

chambers (D1,D2,D3 and D4) at different control rod positions starting from ~ $C_0 / C_i \approx 0.3$ (i.e. counting rate at the end of critical approach by uranium mass) until counting rate $C_0 / C_i \approx 0.01$. The critical height is obtained smoothly by an extrapolation of the (C_0 / C_i) – values.

2.3 Equations of the reactor kinetics at equilibrium

The equations of the reactor kinetics are used to predict the changes in the power level during criticality approach by withdrawal of the control rods [1-2].

$$\frac{\partial n(t)}{\partial t} = [k.(1-b)-1].\frac{n}{u} + l.C + S \tag{2}$$

$$\frac{\partial C(t)}{\partial t} = \frac{k.b.n(t)}{u} - l.C \tag{3}$$

where: $n(t)$ is the neutron density versus time; k – effective neutron multiplication factor; l is the average decay constant of the precursors of the delayed neutrons; C [at.cm^{-3}] is the averaged density of precursors of the delayed neutrons for an averaged single delayed group $b = \sum_{i=1}^{7} b_i$; the total fraction of the delayed neutrons for BR2 is $b_{eff} \approx 0.0072$, including the contribution from photo neutrons [3]; $u = 10^{-4}\,\mathrm{sec}$ is the prompt neutrons life-time; S [n.cm^{-3}.s^{-1}] is the neutron source, inserted into the multiplying medium. At equilibrium Eqs. (3) & (2) become:

$$\frac{\partial C(t)}{\partial t} = 0; \quad \frac{\partial n(t)}{\partial t} = 0 \tag{4}$$

And consequently:

$$C = \frac{k.b.n}{u.l}; \quad 1-k = \frac{S.u}{n} \tag{5}$$

From Eqs. (5) we obtain the following relation between *C* and *k* for two equilibrium levels of the neutron density at positions of the control rods $Sh = Sh_0$ and $Sh = Sh_i$:

$$\frac{C(Sh_i)}{C(Sh_0)} = \frac{C_i}{C_0} = \frac{k_i}{k_0}\left(\frac{1-k_0}{1-k_i}\right) = \frac{r(Sh_0)}{r(Sh_i)} = \frac{r(Sh_0) - r(Sh_{crit})}{r(Sh_i) - r(Sh_{crit})} = \frac{r_0 - r_{crit}}{r_i - r_{crit}} \tag{6}$$

or shortly:

$$\frac{C_i}{C_0} = \frac{r_0 - r_{crit}}{r_i - r_{crit}} \tag{7}$$

where: C_0, C_i – density of the precursors of the delayed neutrons at Sh_i and Sh_0, which can be derived from the measured counts in the fission chambers during approach to criticality; $r(Sh_0 = 300mm) = r_0$ is the excess reactivity at the deepest position of the control rods in montage condition; $r(Sh_{crit}) = r_{crit}$ is the excess reactivity at the critical control rods position.

2.4 Measurements

The following measurements [4] are executed during critical approach by withdrawal of the control rods: (i) measurement of the counts in the fission chambers and determination of $(C_i / C_0)_{meas}$ for different positions Sh_i of the control rods up to the critical position Sh_{crit}; (ii) measurement of the reactor period, i.e. the time T_{crit} for enhancement of the neutron flux density by e times around the critical position $\Delta Sh_{crit} = Sh_{crit} + d$ ($d \approx +8mm$ for typical BR2 loading); (iii) determination of the differential control rod worth at Sh_{crit}, using the in-hour equation:

$$\frac{r_{crit}}{\Delta Sh_{crit}} = \frac{1}{\Delta Sh_{crit}} \left[\frac{u}{k_{eff} T_{crit}} + \sum_{i=1}^{7} \frac{b_i}{1 + l_i T_{crit}} \right] \tag{8}$$

(iv) special measurements for determination of the total worth of a control rod, performed at the BR2 reactor [2]. In these measurements the worth of a control rod is determined by the following procedure: one control rod is removed slowly out of the core from its deepest (fully inserted) to the highest position (totally withdrawn). Few other control rods are moving in opposite direction to compensate the reactivity changes (to keep $k_{eff} = 1.0$). For each step of the control rod movement, the reactor period T_{crit} is measured and the differential worth r_{crit} is determined using the in-hour formula (8); (v) the relative reactivity efficiency of the control rod movement from deepest position Sh_0 (fully inserted) to the highest position (totally withdrawn) are determined using perturbation method [5] by the formula:

$$\frac{r_{crit}}{r_0} = \left[\frac{Sh_{crit}}{Sh_0} - \frac{1}{2p} \sin\left(\frac{2pSh_{crit}}{Sh_0} \right) + \frac{1}{18} \sin^3\left(\frac{pSh_{crit}}{Sh_0} \right) \right] \tag{9}$$

(vi) then from Eqs. (6)-(7) derivation of the reactivity values r_i at each sub-critical position Sh_i.

3 APPROACH TO CRITICALITY IN THE BR2 REACTOR BY MCNPX

The loading for a typical operation cycle of the BR2 reactor contains fuel elements with variable burn up of ^{235}U: from 0% (fresh fuel elements) to 50% burnt fuel elements. Because the core is loaded mainly with burnt fuel elements able to emanate neutrons through fission product decays the insertion of an extraneous neutron source into the BR2 reactor is not necessary. An additional source of neutrons comes also from the (γ,n) – reactions on the beryllium matrix, in which the fuel elements are positioned. Therefore, the approach to criticality in the BR2 reactor is maintained without extraneous neutron source, using the delayed neutrons and photo neutrons as a neutron source. An extraneous source has been inserted into the core at the first criticality of the reactor BR2 in 1962 (the core has been loaded with fresh fuel and therefore there was no source of delayed γ – rays in the reactor).

3.1 Initial neutron source used with MCNPX

The Monte Carlo code MCNPX [6] is used to predict the reactivity values and counts in the detector (fission chamber) in function of control rods position during approach to criticality. Two types of neutron source are available in the MCNPX code: (i) fission source – automatic criticality calculation of k_{eff}, the eigenvalue to the neutron transport equation, when the initial neutrons start from the fission assemblies; (ii) fixed extraneous neutron source – in this case the user introduces the desired energy and spatial source distribution; the output of the MCNP run is the net multiplication factor of the system *M*, which is used to estimate k_{eff}^{FS} (calculation with Fixed Source). In general k_{eff}^{FS} differs from k_{eff} in the criticality calculation, unless the fixed source distribution is identical in space and energy to the source distribution obtained from the solution of the eigenvalue problem with $k_{eff} < 1$. The relation between the net multiplication factor *M*, obtained from a fixed source run and k_{eff}, obtained from the criticality calculations is given by [6]:

$$M = \frac{1 - \frac{k_{eff}}{\bar{n}} + G_x^0}{1 - k_{eff}} \tag{10}$$

Where: $\bar{n}$ is the average number of neutrons, emitted per fission event; G_x^0 is the non-fission multiplicative reaction, obtained in the criticality calculation.

3.2 Reactivity as function of control rod position

MCNPX simulation calculations of k_{eff} are performed for different position Sh_i of the control rods during the critical approach at six BR2 operation cycles. The both source options available in MCNP are used in the calculations. Because the critical approach in BR2 is carried out without an extraneous neutron source, it is natural to use the fission source in MCNP with neutrons started from the fission assemblies. However, with a purpose of comparison, similar calculations have been simulated with an external neutron source having Maxwell fission spectrum and distributed in a few burnt fission assemblies around the core center. The results of the calculations are given in Fig. 1. As can be seen the uses of the both sources – fission and external neutron source – give similar results for the changing of reactivity values with the withdrawal of the control rods from the sub-critical core.

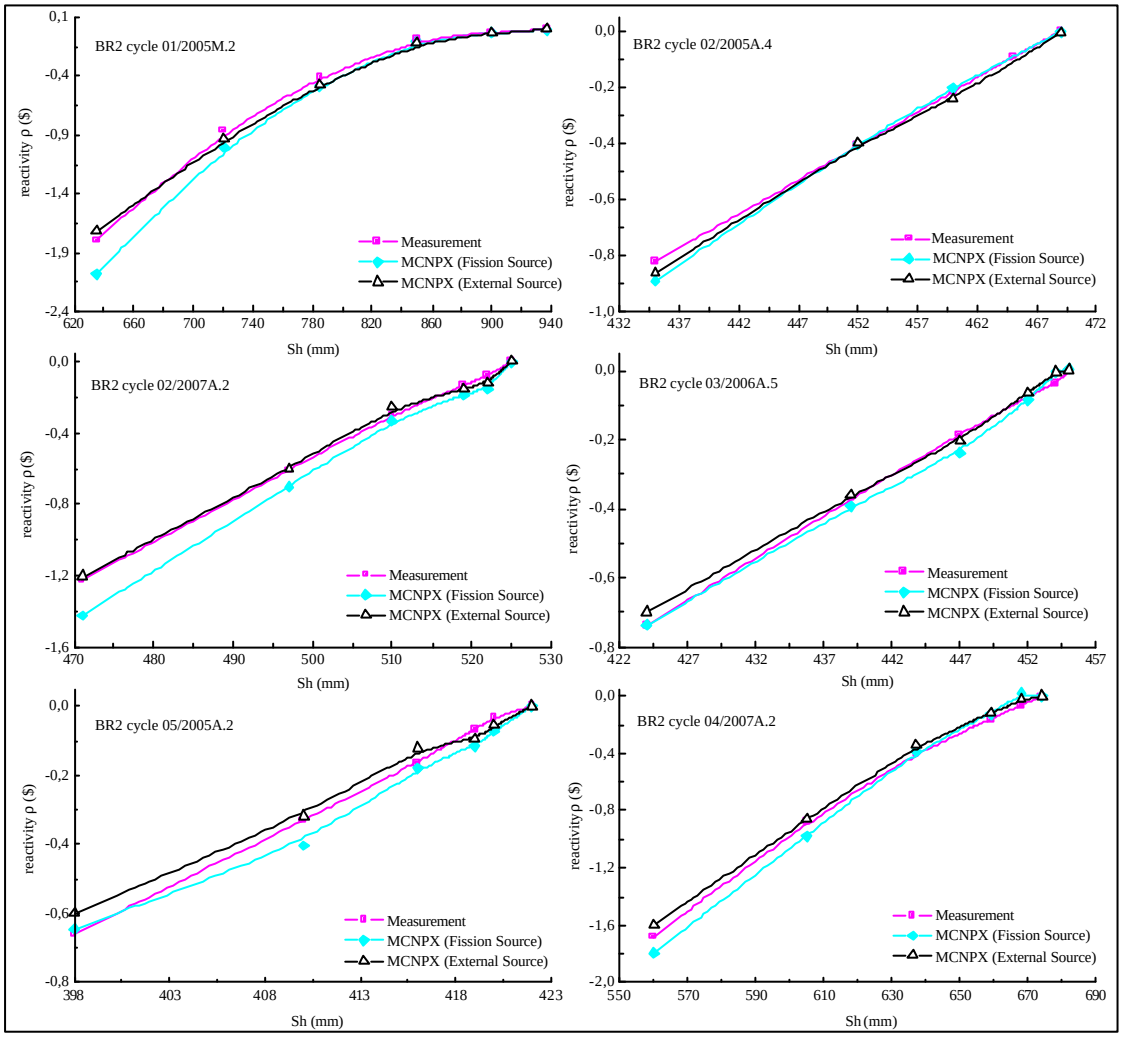

Figure 1 Comparison of measured and calculated reactivity values during critical approach in BR2 sub-critical core, using two available neutron source options in MCNP – fission source and external source having Maxwell spectrum and distributed in the burnt fuel elements.

3.3 Prediction of the counts in the detector using MCNPX & Point Kinetics

A simple hybrid MCNPX & Point Kinetics method is applied to predict the counts in the fission chamber as function of control rods position during their removal from the core at approach to criticality in the BR2 reactor. The following calculation procedure is implemented: (i) detailed calculations by MCNPX of the total control rod worth for an arbitrary BR2 operation cycle and

arbitrary burn up of the lower cadmium section of the active part of the Reference Control Rod; (ii) normalization of the curve of the total control rod worth to unity (see Fig. 2a) and validation on the measurements of total control rod worth, performed at the BR2 reactor; (iii) plot of the graphs C_i / C_0 as function of control rod position $Sh(I)$ for different critical heights $Sh(crit)$ using the kinetic equation (7) in the following form:

$$\frac{C[Sh(I)]}{C[Sh(300)]} = f[Sh(I)] = \frac{r[Sh(300)] - r[Sh(crit)]}{r[Sh(I)] - r[Sh(crit)]} \qquad (11)$$

This results in a series of plots for different critical control rods positions (see Fig. 2b), which are obtained using only the data for the relative rod efficiency from Fig. 2a; (iv) the final step is to use the plots, given in Fig. 2b to predict the counts in the detector (fission chamber) during approach to criticality in the reactor BR2 by withdrawal of the control rods.

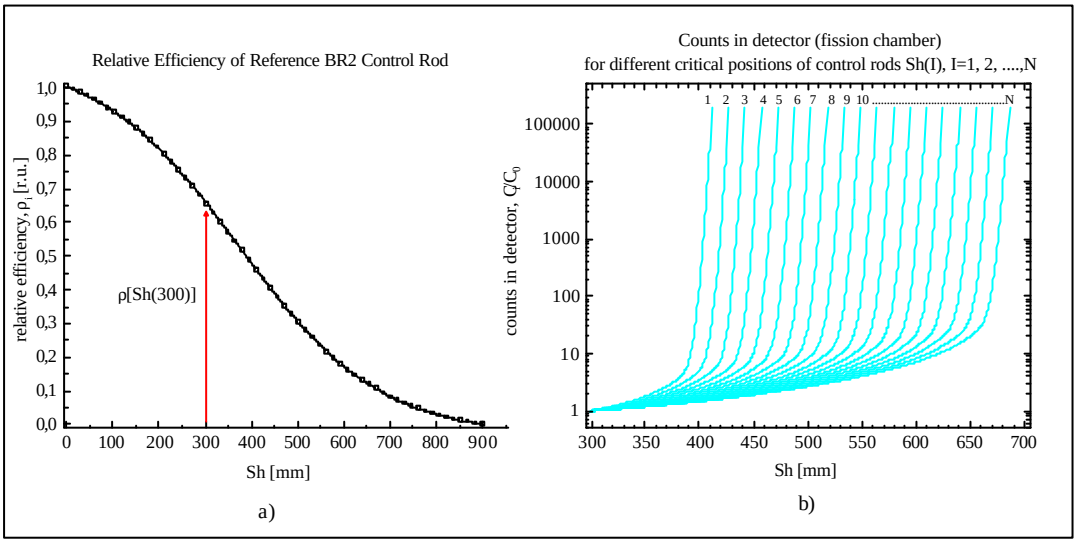

Figure 2 a) Relative efficiency of reference control rod in the BR2 reactor; b) plots of the counts in the detector (fission chamber) for different critical positions of the control rods.

The described above simple procedure for prediction of the counts in the fission chamber has been verified on six BR2 operation cycles. This assumes that we perform only one, but accurate criticality calculation to determine the value of the critical rods position $Sh(crit)$ for the considered reactor core load. Then for the determined $Sh(crit)$ we can easily use one of the plots given in Fig. 2b to estimate the changes in the neutron flux level with removal of the rods out of the sub-critical core. The application of such technique for the prediction of the counts in the detector has been compared with the measurements during approach to criticality in several BR2 operation cycles, which is demonstrated at Fig. 3 As it can be seen the agreement

between the calculated and the measured counts in the sub-critical core is perfect. However, it is obvious that for an inaccurate determined critical position, the calculated (predicted) curves of the counts in the detector will be left- or right- shifted relatively to the measurement curves. The main uncertainties in the predicted counts in the fission chamber at critical approach in a highly heterogeneous reactor like BR2 result from the adequacy of geometry and material description and used neutron interactions data in determination of $Sh(crit)$.

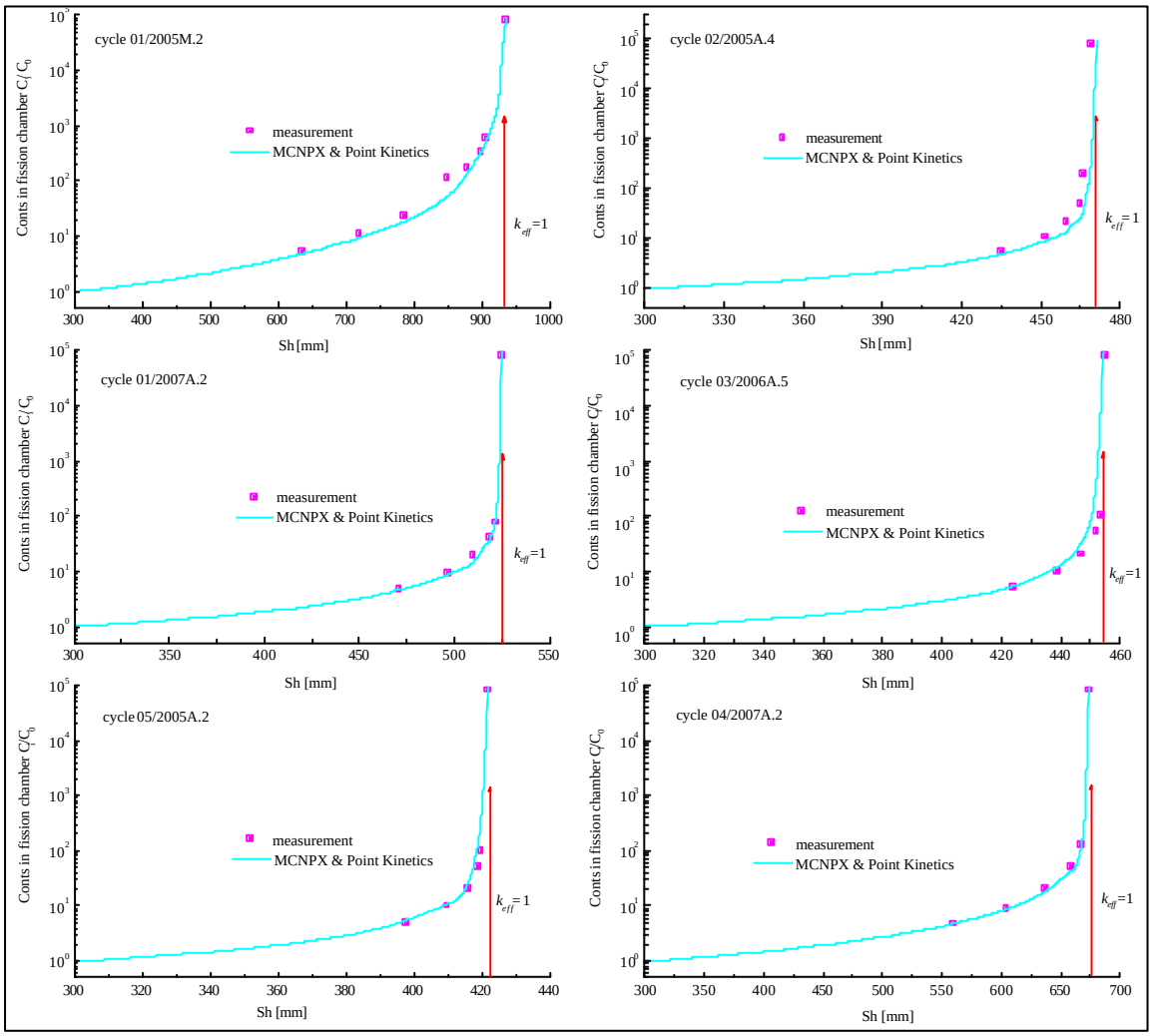

Figure 3 Comparison of the calculated counts in a neutron detector (fission chamber) using MCNPX&Point Kinetics method with the measurements during critical approach in the BR2 sub-critical core.

4 CONCLUSIONS

The Monte Carlo code MCNPX has been used in combination with point kinetics method to study the behavior of the sub-critical core during approach to criticality in the BR2 reactor by withdrawal of the control rods. The application of a fission source or an external neutron source having Maxwell spectrum and distributed in few burnt fuel assemblies around the core center has given similar results for the changing of the relative neutron density level (reactivity) in the sub-critical core. This has been expected since the BR2 reactor does not use an explicit extraneous neutron source at the critical approach. The neutron source needed for the sub-critical counting is provided by the delayed neutrons from the burnt fuel assemblies and by the photo neutrons from the beryllium matrix. A simple hybrid MCNPX & Point Kinetics method has been implemented in support of the experimental technique for prediction of the counts in the detector (fission chamber) used to monitor the neutron flux level during the critical approach. The method uses the curve of the relative control rod efficiency, which is calculated only once for an arbitrary BR2 cycle with an arbitrary burn up of the lower cadmium part of the Reference Control Rod. Before the critical approach only one Monte Carlo simulation calculation must be performed by MCNPX in order to determine the critical height for the reactor core load of the considered operation cycle. Then using the reactor kinetic equations we can easily derive the counts in the detector (fission chamber). The application of the simple hybrid method has shown an excellent agreement between the calculated and measured counts in the detector. However, the authors recognize that the main difficulties of the proposed method are associated with the uncertainties of the calculated critical rod position resulting from the non-adequate geometry or material description in the Monte Carlo simulation run.

5 REFERENCES

1. M.A.Schultz, "Control of Nuclear Reactors and Power Plants", Westinghouse Electric Corporation, Pittsburgh, Pennsylvania, 1961.
2. A.Beeckmans, "Reactor Response for a Step of Reactivity of 0.20 $", D27010/ABW/282, BR2 Reactor, SCK-CEN, Mol, Belgium, 19/05/1999.
3. W.Rotter, "Verzogerte Photoneutronen im Beryllium-Reaktor BR 02", *Nukleonik*, 5. Band, 6. Heft, 1963, S.227-236. Springer-Verlag, Berlin.
4. B.Ponsard, “Period Measurements Before Start Up Of the Reactor BR2 Cycles”, A001070/BP/2007, BR2 Reactor, SCK-CEN, Mol, Belgium.
5. G.M.Schindler, "On the Efficiency of A Concentric Cut-Off Rod of A Thermal Reactor as A Function of the Inserted Length of the Rod", *J. Nuclear Energy,* Vol. 8, pp. 18 to 32. Pergamon Press Ltd., London.
6. MCNP/MCNPX, Monte Carlo N-Particle Transport Code System. Oak Ridge National Laboratory, RSICC Computer Collection, November (2005).

MODELLING OF A PROMPT GAMMA NEUTRON ACTIVATION SYSTEM FOR CHARACTERISATION OF RADIOACTIVE MATERIALS

J.KETTLER*, R. NABBI, E. MAUERHOFER
Institute of Energy Research - Safety Research and Reactor Technology IEF-6
Leo-Brandt-Straße, 52425 Jülich, Research Centre Jülich, Germany

**J.Kettler@fz-juelich.de*

ABSTRACT

A simulation study of a Prompt Gamma Neutron Activation Analysis (PGNAA) system with a 14 MeV neutron generator was carried out using the MCNP-5 Monte-Carlo-Code to investigate the correlation between the gamma emission rate of certain elements and the hydrogen concentration in a large concrete sample.
The experimental hall with the PGNAA system and the surrounding labs were modelled in detail to calculate the dose rates at various locations of interest with the MCNP dose function and data from ICRP 60.

1. Introduction

Low and intermediate radioactive waste (LILW) may contain toxic materials like heavy metals. The final storage of LILW containing such toxic components must comply with the regulations defined by the German authority and their properties need to be taken into account for a safe disposal. Thus the amount and type of chemically toxic elements in radioactive waste must be determined or checked. For this aim a non-destructive method based on Prompt Gamma Neutron Activation Analysis (PGNAA) with a 14 MeV neutron generator will be developed at the Institute of Energy Research of Research Centre Jülich.
The PGNAA is an analytical technique which is based on the gamma spectrometric detection of prompt gamma radiation emitted simultaneously due to the neutron capture (Figure 1). In comparison to conventional Neutron Activation Analysis (NAA) no knowledge of the half-life of the radionuclide is necessary that allows the identification and characterization of any number of elements existing in the samples [1] [2].
This paper reports the results of MCNP [3] simulations, carried out to study the variation of gamma emission rate of some selected elements by varying the hydrogen content in a reference concrete sample. Furthermore for the aim of radiation protection the MCNP model was used to determine the dose rate around the PGNAA device.

2. Experimental Setup

The PGNAA drum assay system consists of a graphite interrogation chamber, a deuterium-tritium (D-T) accelerator neutron source (of 14 MeV energy and 10^8 n/s strength) [4] for the irradiation of the waste drum and a high-purity n-type Germanium (HPGe) detector for the measurement of prompt gamma radiation yield. The wall of the graphite chamber is approximately 40 cm thick, which is used as a shield to protect the environment of the experiment against neutrons as well as a reflector. In order to reduce fast neutron damage the detector is arranged perpendicularly to the neutron generator. As reference sample a 40 x 40 cm steel drum homogeneously filled with dry concrete will be used for the analysis with PGNAA. The PGNAA drum assay system will be set up in a 12 m x 4.8 m experimental hall with 85 cm thick baryta concrete walls.

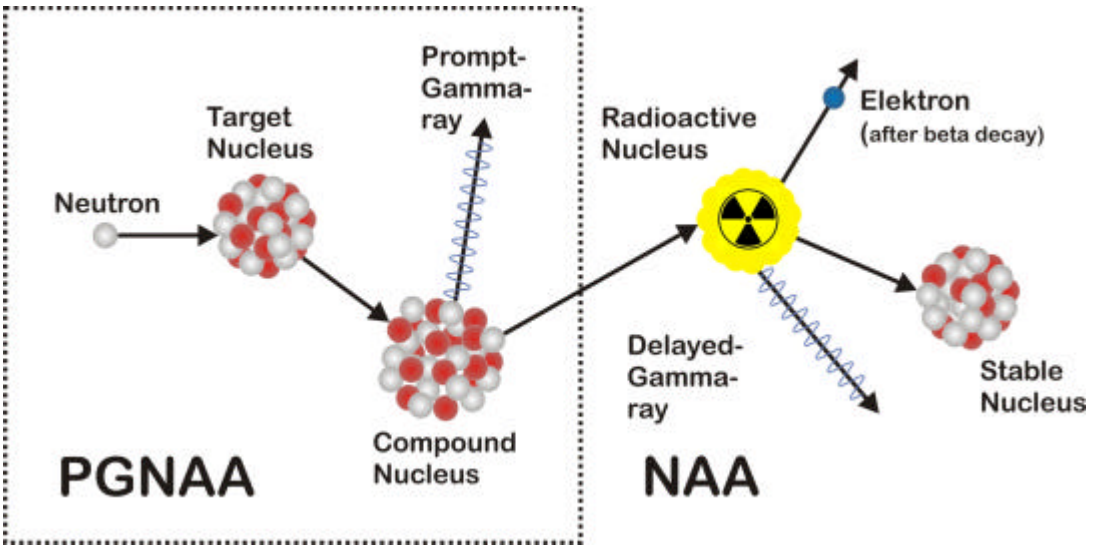

Fig. 1 The reaction scheme shows the different between PGNAA and NAA. The time between neutron capture and emission of the prompt gamma ray ranges from 10^{-12} - 10^{-16} s.

3. Computational method

The MCNP model of the PGNAA system given in Figure 2 consists of the three main parts described above. Using the MCNP-5 Monte-Carlo Code and the libraries ENDF/B-VII respectively JEFF 3.1 simulations were performed to optimize the experimental setup. In the MCNP input-file a slab geometry is assumed for the neutron source isotropically emitting 10^8 neutrons per second in 4π sr. The detector crystal is represented by a 4.77 cm x 14.76 cm cell containing natural Germanium (pulse height tally), where the track length of gamma rays are simulated like in a real HPGe-detector. For the detector simulation the JEFF-3.1 neutron and radiation data library was employed. The sample is a 0.2 cm thick steel drum, homogenous filled with dry concrete (approx. 115 kg). The weight composition is presented in table 1.

Tab. 1 Composition of the dry concrete

Element	Fraction [w%]	Element	Fraction [w%]	Element	Fraction [w%]	Element	Fraction [w%]
H	0.5558	Al	4.5746	Ca	8.2941	Na	1.7101
O	49.8076	Si	31.5092	Fe	0.2147	Mg	0.2565
K	1.9239	S	0.1283				

In order to simulate samples with higher H-content, the fraction of oxygen was continuously replaced by hydrogen. To optimize the setup of the PGNAA-system the prompt gamma spectrum and the neutron flux at the detector surface were first investigated for different detector/ neutron source configurations. For the dose rate calculations the experimental hall with the surrounding labs was modelled in detail. The simulations were performed using the MCNP dose function as well as data from ICRP 60. In every simulation run 10^9 particle histories were calculated resulting in high statistical precision in term of relative error and variance of variance (vov), which remained within the accuracy intervals (1 σ value of 0.2%)

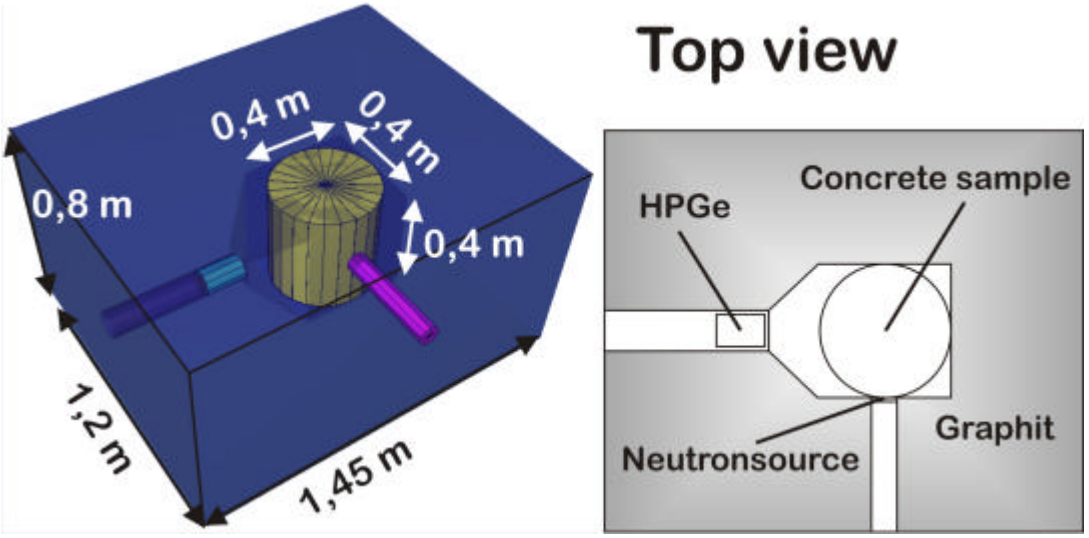

Fig. 2 Schematic setup of the PGNAA system with neutron source and HPGe crystal.

4. Results and discussion

The dependence of the gamma emission rate for Al (7.725 MeV), Si (4.935 MeV) and H (2.223 MeV) with the H-concentration of the concrete sample is shown in Figure 3. Accordingly the count rate increases linearly for a H concentration lower than 1.6 w%. A further increase of the H-concentration in the sample leads to an exponential decrease of the gamma activity of aluminium and silicon due to the thermal neutron capture by hydrogen. This finding is in agreement with the result of reference [5]. In the case of hydrogen the gamma yield decreases linearly due to of the increase of hydrogen concentration. The dependence of the gamma emission rate of C (4.945 MeV) in the graphite chamber with the H-concentration of the sample is shown in Figure 4. We observed that the gamma count rate of C decreases for an increasing H-concentration as a result of the moderation of the fast neutrons in the sample. Consequently the signals of C and H are appropriate for monitoring the mean thermal flux in the sample.
Neutron and photon dose rates were calculated for radiation protection purposes at various locations around the experimental hall for two configurations of the PGNAA device (Figure 5). The results shown in table 2 demonstrate that the photon dose rates are negligible in comparison to the contribution of neutrons. The neutron dose rates depend on the alignment of the PGNAA device i.e. on the orientation of the neutron generator. For the existing configuration the calculated dose rates remain below 2,3 µSv/h, that is prescribed by Federal Office for Radiation Protection (BfS) as a limit for a radiation exposed working person.

Tab. 2 Neutron and photon dose rates at different places of interest (see Fig. 5.)

Place of interest	**Neutron dose rate [mSv/h]**		**Photon dose rate [fSv/h]**	
	Orientation 1	**Orientation 2**	**Orientation 1**	**Orientation 2**
Outside of the sliding gate – 1	0.0346	0.3113	0.00045	0.00148
Way of walking outside of the hall – 2	0.0179	0.0083	0.00019	0.00012
Adjoining laboratory – 3	0.0050	0.0153	0.00021	0.00039
Lead window to look inside the hall – 4	0.0236	0.0104	0.00022	0.00011

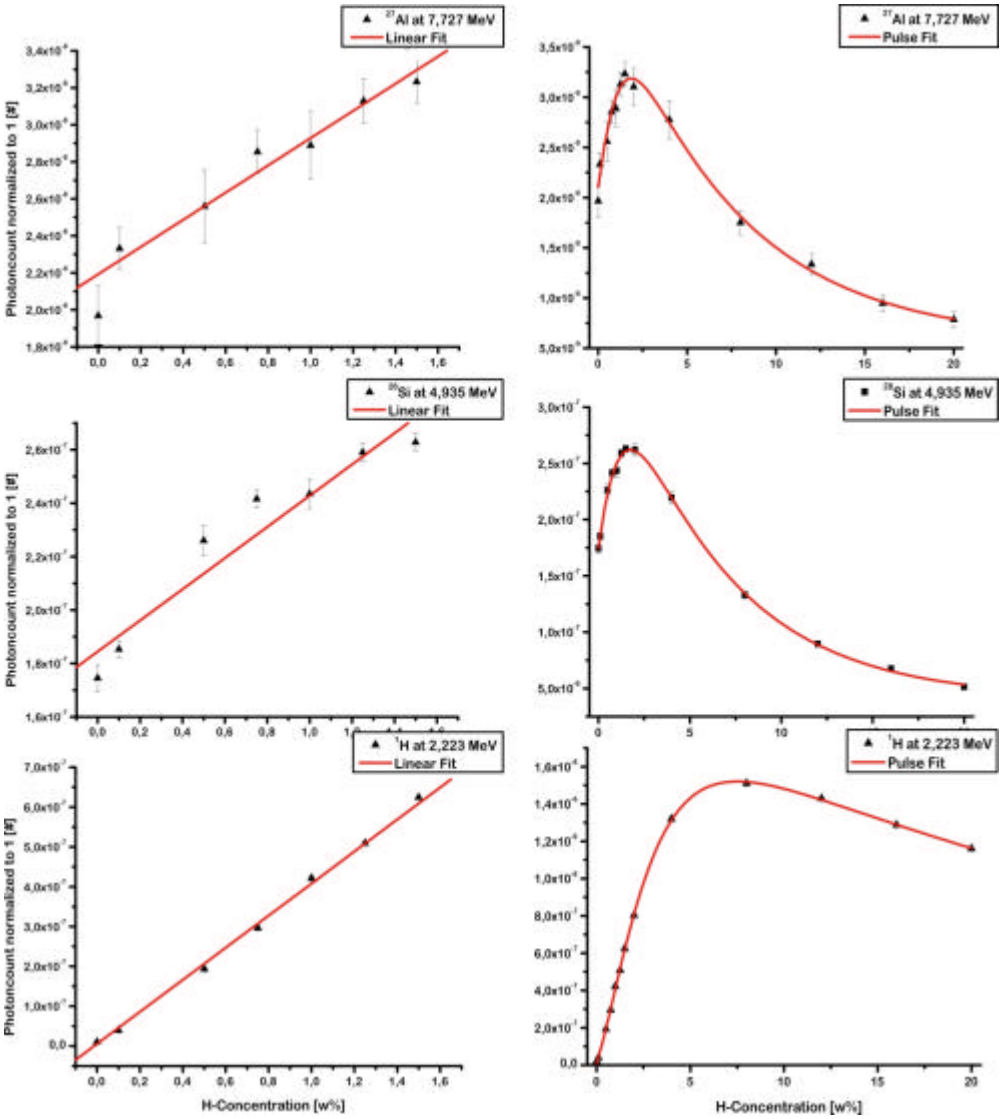

Fig. 3 Gamma count rates of aluminium, silicon, and hydrogen as a function of the H-concentration in the concrete sample.

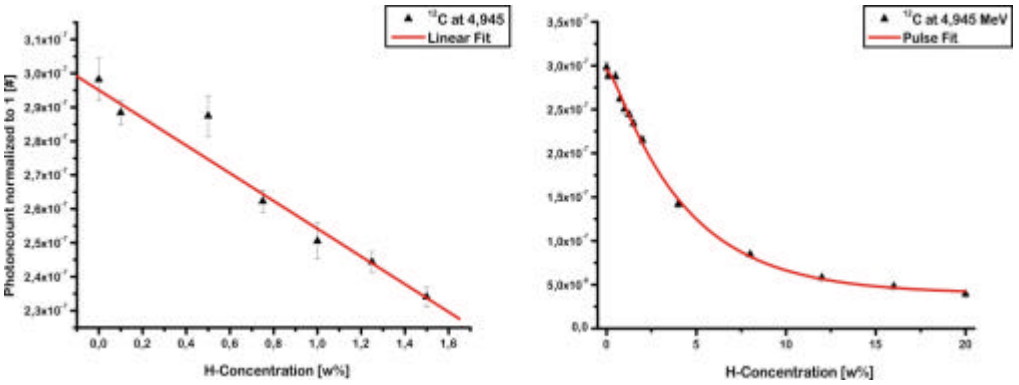

Fig. 4 Gamma count rate of the carbon in the graphite chamber as a function of the H-concentration in the concrete sample.

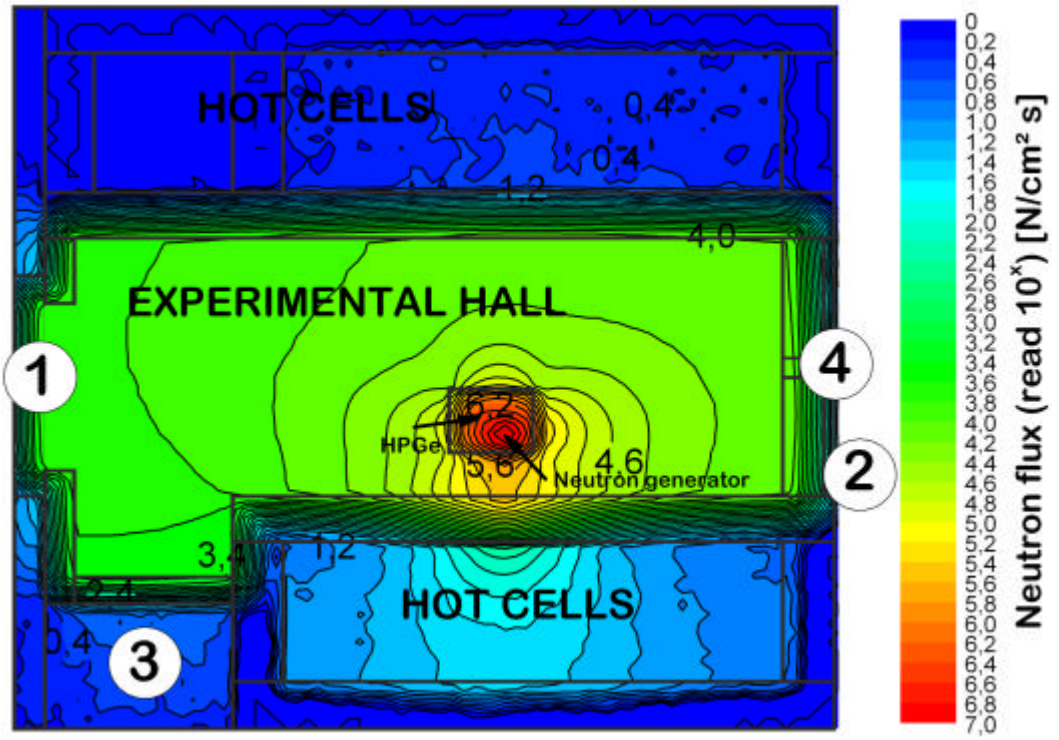

Fig. 5 Total neutron flux (0 - 14 MeV) contour plot for the PGNAA device (Orientation 1) in the experimental hall. The scale values are the exponents of the neutron flux (7 reads as 10^7). The location of the dose rate calculations are given by the number in the circles (see Tab. 2). In Orientation 2 the PGNAA model of the measurement setup was 90° rotated in clockwise direction relative to Orientation 1.

5. Conclusions

For the certain elements selected in this work for coupled neutron and gamma transport analysis a linear correlation between the gamma emission rate and a hydrogen concentration in the sample was determined for the concentration range of 0 – 1.6 w%. For higher concentrations the gamma count rate decrease exponentially due to the increasing neutron capture of hydrogen. Dose rate calculations with MCNP-5 using the activation and gamma data library ENDF/B-VII and JEFF 3.1 show that the radiation exposure at various locations outside the experimental hall are lower than the limits set by the Federal Office for Radiation Protection.

6. References

[1] KEISUKE, S. ; KOBAYASHI, K. ; SATO, W. ; NAKAHARA, H. ; TOMIZAWA, T.: Nondestructive Determination of Major Element in a Large Sample by Prompt Gamma Ray Neutron Activation Analysis. *In: Analytical Chemistry* 68 (1996) No. 13, S. 2203-2209

[2] MOLNÁR, Gábor L.: *Handbook of Prompt Gamma Activation Analysis.* Budapest: 1. edition Kluwer Academic Publishers, 2004. - 1-4020-1304-3

[3] X-5 Monte Carlo Team: *MCNP - A General Monte Carlo N-Particle Transport Code, Version 5.* Los Alamos National Laboratory: 2003.

[4] EADS-SODERN: *Neutron Generator GENIE 16 GT.* http://www.sodern.fr

[5] OLIVEIRA, C. ; SALGADO, J. ; CARVALHO, F. G.: Optimation of PGNAA instrument design for cement raw materials using the MCNP code. *In: Journal of radioanalytical and nuclear chemistry* 216 (1997) No. 2, S. 191-198

European Nuclear Society
Rue de la Loi 57
1040 Brussels, Belgium
Telephone +32 2 505 30 54
Fax + 32 2 502 39 02
rrfm2008@euronuclear.org
www.euronuclear.org